Identification of a Highly Functional Effector CD8$^+$ T Cell Program after Transplantation in Mice and Humans

Gregory S. Cohen,[1†] Joel S. Freibaum,[1†] Riley P. Leathem,[1†] Marina W. Shirkey,[2] Robin Welsh,[1] Ryo Hatano,[3] Chikao Morimoto,[3] Byoung Chol Oh,[4] Daniela Čiháková,[1,5] Jonathan S. Bromberg,[6] Scott M. Krummey[1*]

[1]Department of Pathology, Johns Hopkins School of Medicine, Baltimore, MD, 21205, USA

[2]University of Maryland School of Medicine, Department of Surgery, Center for Vascular and Inflammatory Diseases, Baltimore, MD, 21201, USA

[3]Department of Therapy Development and Innovation for Immune Disorders and Cancers, Graduate School of Medicine, Juntendo University, Tokyo 113-8421, Japan

[4]Department of Plastic and Reconstructive Surgery, Johns Hopkins School of Medicine, Baltimore, MD, 21205, USA

[5]W. Harry Feinstone Department of Microbiology and Immunology, Bloomberg School of Public Health, Johns Hopkins University, Baltimore, MD, 21205, USA

[6]University of Maryland School of Medicine, Departments of Surgery and Microbiology and Immunology, Center for Vascular and Inflammatory Diseases, Baltimore, MD, 21201, USA

†These authors contributed equally to this work.

*Corresponding Author: Scott M. Krummey, Ross Research Building Room 664B, 720 Rutland Avenue, Baltimore, MD 21205, 410-955-3600, skrumme1@jhmi.edu

Word count: 3,967

Keywords: effector CD8$^+$ T cells, alloimmunity, costimulation blockade, tolerance

ABSTRACT

T cell mediated allograft rejection leads to early graft loss for kidney transplant patients. To better understand the mechanism by which T cells mediate rejection, we investigated the fate and function of graft-specific $CD8^+$ T cells expressing the activated isoform of CD43 in mice and humans. Agonism of CD43 1B11 in vitro induced $CD8^+$ T cell proliferation in the presence of sub-threshold antigen stimulation, and CD43 1B11 mAb treatment in vivo overcame costimulation-blockade induced tolerance to skin grafts. Relative to CD43 $1B11^-$ populations, CD43 $1B11^+$ $CD8^+$ T cells maintained high T-bet expression along with stem-like molecules IL-7Rα and TCF-1 at both effector and memory timepoints, and were more persistent following adoptive transfer. In kidney transplant patients, graft-infiltrating $CD8^+$ T cells that expressed CD43 and the glycosyltransferase GCNT1 had an effector phenotype that includes high expression of *IFNG*, *ICOS*, and perforins/granzymes. In healthy human donors and transplant candidates, the CD43 1D4 mAb clone defined antigen-experienced cytokine-producing $CD8^+$ T cells. In sum, these data support a progressive differentiation model by which highly proliferative effector CD43 $1B11^+$ $CD8^+$ T cells infiltrate allografts also efficiently persist into memory after antigen clearance.

45 **1. INTRODUCTION**

46

47 T cell mediated allograft rejection is a major contributor to early graft loss.[1–3] Multiple
48 studies have highlighted that CD8$^+$ T cells, which have potent cytolytic and cytokine-producing
49 functions, mediate rejection in pre-clinical models and patients.[4–8] In the widely held early
50 precursor model of T cell differentiation, CD8$^+$ T cells become either short-lived effector cell
51 (SLEC) populations or longer-lived memory precursor populations in the initial cell divisions after
52 antigen priming. Following viral and bacterial infection, the transcription factor T-bet is essential
53 for CD8$^+$ T cell effector function of short-lived effectors, but also sustains memory cell
54 homeostasis.[10,16,17] In parallel, self-renewing stem-like features of CD8$^+$ T cell memory are defined
55 by responsiveness to IL-7 and the transcription factor T cell factor 1 (TCF-1).[18–20] While many
56 features of effector and memory CD8$^+$ T cells have been described, the allogeneic priming
57 environment differs significantly from that of pathogen infection.[11,13,21,22] The overarching model of
58 CD8$^+$ T cell differentiation in transplantation is not well understood.

59 CD43 is a transmembrane sialomucin which is broadly expressed on leukocytes, and has
60 complex functions in cellular adhesion and trafficking, as well as cellular signaling.[23–26] However,
61 T cell activation elicits the core-2 O-glycosylation of CD43 by the glycosyltransferase GCNT1, [27,28]
62 which is denoted by the binding of the CD43 1B11 antibody clone. Our group and others have
63 shown that effector and memory CD8$^+$ T cells upregulate expression of the activated CD43
64 receptor.[23,29,30] We found that after transplantation, CD43 1B11 CD8$^+$ T cells were potent effectors
65 that expressed highly levels of Granzyme B, the cytokines IFN-γ/TNF-α, and rapidly infiltrated
66 allografts.[29] In the present study, we further delineated key aspects of the fate and function of this
67 CD8$^+$ T cell population in mice and humans in order to better understand the population dynamics
68 driving T cell mediated rejection.

69

70

71 **2. MATERIALS AND METHODS**

72

73 **Animals.** C57BL/6J, C57BL/6J Ly5.2-Cr (CD45.1), C57Bl/6-Tg(TcraTcrb)1100Mjb/J (OT-I), and
74 C567BL/6-Tg(CAG-OVAL)916Jen/J (Act-mOVA) were obtained from The Jackson Laboratory
75 (Bar Harbor, Maine) and used at 6-12 weeks of age. Balb/cJ, were obtained from The Jackson
76 Laboratory and bred at Johns Hopkins University. This study was conducted in accordance with
77 the recommendations in the Guide for the Care and Use of Laboratory Animals, and was approved
78 by the Animal Care and Use Committee at Johns Hopkins University. Animals were housed in
79 specific pathogen-free animal facilities at Johns Hopkins University.

80

81 **Skin transplantation and in vivo treatments**. Full-thickness tail and ear skins were transplanted
82 onto the dorsal thorax of recipient mice and secured with adhesive bandages as previously
83 described [31]. In some experiments, mice were treated with 250 μg/dose of CTLA-4 Ig (BioXCell)
84 and anti-CD40L (MR1 clone, BioXCell) via i.p. injection as indicated. CD43 1B11 mAb (Biolegend)
85 was provided at 200 μg/dose via i.p. injection.

86

87 **Heart transplantation and graft-infiltrating T cell isolation.** Heterotopic heart allografts were
88 performed as previously described via anastomosis to the abdominal aorta and pulmonary
89 artery.[32] To isolate graft-infiltrating cells, heart grafts were perfused with 1x PBS for 5 min, then
90 minced and digested using Collagenase II (5000 U/mL) and DNase I (500 U/mL) (Worthington
91 Biochemicals) in HBSS (Corning) for 30 min at 37 C with gentile agitation. Tissue was then
92 dissociated using a GentleMACS Tissue Dissociator (Miltenyi).

93

94 **Flow cytometric cell sorting and adoptive transfer**. To obtain effector $CD8^+$ T cells,
95 splenocytes and graft draining lymph nodes (inguinal, brachial, axial) from $CD45.1^+$ mice grafted

96 with Balb/c skin grafts 10-14 days prior were collected and processed to single cell suspension.
97 For proliferation analysis, $2x10^6$ $CD8^+$ T cells were isolated using $CD8^+$ T cell negative selection
98 kit (Miltenyi), and stained with CellTrace Violet (Invitrogen) prior to adoptive transfer. For fate
99 experiments, effector $CD8^+$ T cells were flow cytometrically sorted into $CD44^{hi}CD62L^{lo}CD8^+$ T cells
100 that were CD43 $1B11^+$ and CD43 $1B11^-$ using a MoFlo XDP instrument. 0.9-$1.2x10^5$ purified cells
101 were transferred via tail vein into C57BL/6J mice. Mice were grafted the following day with Balb/c
102 skin and analyzed by flow cytometry on the indicated day post-graft as described below.
103
104 **In vitro T cell stimulation**. 96-well flat-bottom tissue culture plates were coated with CD3ε, CD28,
105 or CD43 1B11 mAb (Biolegend) at the indicated concentration in 60 μL of PBS/well for 90 min at
106 37 C. Naïve $CD8^+$ T cells isolated using $CD8^+$ T Cell Isolation Kit with LS columns (Miltenyi) were
107 stained with CellTrace Violet (Invitrogen). $2x10^5$ $CD8^+$ T cells were plated per well and incubated
108 at 37 C for 4 days in Complete R10 media comprised of RPMI 1640 with L-glutamine (Corning),
109 10% FBS, 100 mM HEPES, 500 uM β-mercaptoethanol, 100 U/mL penicillin/stremptomycin and
110 analyzed by flow cytometry as described below.
111
112 **Immunofluorescence microscopy.** Draining lymph nodes (dLN) were flash frozen in OCT
113 compound (Sakura Finetek, Torrance, CA). Six µm sections were cut in triplicate using a Microm
114 HM 550 cryostat (Thermo Fisher Scientific), fixed in cold 1:1 acetone:methanol for 5 minutes, and
115 washed in PBS. Slides were incubated in primary antibodies and secondary antibodies diluted in
116 PBST (PBS + 0.03% Triton-X-100 + 0.5% BSA) for 1 hour each. Slides were imaged using an
117 Accu-Scope EXC-500 fluorescent microscope (Nikon, Tokyo, Japan). Images were analyzed with
118 Volocity software (PerkinElmer, Waltham, MA). Mean of mean fluorescence intensity (MFI) was
119 calculated within demarcated high endothelial venule (HEV) region. Groups were compared using

120 quantitation of MFI multiplied by percent area (sum of HEV area with fluorescence over total HEV
121 area x MFI).
122
123 **Murine T cell enrichment and flow cytometry**. Flow cytometry and magnetic bead enrichment
124 were performed in 1X PBS (without Ca^{2+}/Mg^{2+}, pH 7.2), 0.25% BSA, 2 mM EDTA, and 0.09%
125 azide. CD45.1^{+} or L^{d} QL9^{+} CD8^{+} T cells were enriched using magnetic beads specific for
126 fluorophores with LS columns (Miltenyi). MHC tetramers with human β2-microglobulin specific for
127 QL9 (H-2L^{d} QLSPFPFDL) were obtained from the NIH Tetramer Core facility. Single cell
128 suspensions were stained with Live/Dead NIR Zombie (Biolegend) and incubated with the
129 indicated antibodies for 30-60 min at room temperature. Intracellular staining was performed using
130 the Transcription Factor Staining Kit (eBiosciences). Samples were acquired on a Cytek Aurora
131 (4L or 5L configuration).
132
133 **Human peripheral blood cell analysis.** Healthy donor peripheral blood was collected in
134 Vacutainer tubes containing sodium heparin (BD Biosciences) and processed according to
135 manufacturer's instructions to isolate mononuclear cells. For cytokine production, 1.0×10^{6} PBMC
136 were plated in 96 well U-bottom plates in complete RPMI with L-glutamine (10% FBS, 10 mM
137 HEPES, 10 μM β-mercaptoethanol) for 20 h at 37 C. T cells were stimulated with 0.5 μg/mL CD3ε
138 mAb (OKT3; ThermoFisher) for 20 hrs at 37 C in the presence of 10 μg/mL GolgiStop
139 (ThermoFisher). For flow cytometry, $0.5\text{-}1.0 \times 10^{6}$ PBMC were stained with Live/Dead NIR Zombie
140 (Biolegend), incubated with supernatant from 1D4 hybridoma for 30 min, followed by anti-mouse
141 IgG PE, and the remaining surface antibodies as indicated. Intracellular staining was performed
142 using the Transcription Factor Staining Kit (eBiosciences) with TNF-α and IFN-γ antibodies.
143 Samples were acquired on a Cytek Aurora (4L and 5L) instrument.
144

145 **Human scRNAseq kidney transplant biopsy analysis**. Biopsies were collected from kidney
146 transplant patients experiencing acute rejection as described.[33] Gene count matrices for the
147 samples were generated by CellRanger count, and analyzed in R (4.3.0) using Seurat (4.3.0.1).
148 Cells with excluded with fewer than 200, more than 2500 gene counts, or greater than 20%
149 mitochondrial DNA. Analysis was filtered on mature $CD8^+$ T cells defined as cells expressing at
150 least one chain of CD3, CD8A, and not expressing CD4. The samples were integrated using the
151 top 2000 genes and 50 dimensions. Dimensionality reductions and clustering analysis were
152 generated using the first 12 dimensions and a resolution of 0.5. Relevant figures were
153 generated with ggplot2 (3.4.3) and pheatmap (1.0.12).
154
155 **Quantification and Statistical Analysis**
156 ***Statistical Analysis*.** All data points represent individual mice, and where individual data points
157 are not depicted the value of n is provided in the corresponding figure legend. For analysis of
158 absolute numbers and expression levels, paired or unpaired Student's t-tests (two-tailed) were
159 performed between two groups; one-way or two-way ANOVA with multiple comparison tests were
160 used to compare multiple groups. Log-rank (Mantel-cox) test was used to evaluate graft survival
161 between groups. Error bars represent standard error measurements (SEM). Statistics were
162 performed using GraphPad Prism 9 or 10. Significance was determined as *$p<0.05$, **$p<0.01$,
163 ***$p<0.001$, ****$p<0.0001$.
164
165 **Study Approval**. Healthy donors and kidney transplant candidates were isolated following
166 protocols approved by the Johns Hopkins Institutional Review Board.
167

168 **3. RESULTS**
169

170 **3.1 CD43 1B11 agonism with mAb provides costimulatory signal to CD8$^+$ T cells**

171 Published studies with multiple experimental systems and reagents have demonstrated
172 that the CD43 receptor can provide either costimulatory or inhibitory signals to T cells.[25,34,35] We
173 stimulated purified CD8$^+$ T cells with a range of plate-bound CD3ε and CD28 mAb in the
174 presence or absence of plate-bound CD43 1B11 mAb **(Figure 1A)**. We found that a
175 concentration of 10 μg/mL CD3ε/CD28 elicited uniform proliferation of CD8$^+$ T cells **(Figure 1A)**,
176 while 0.625 μg/mL of CD3ε/CD28 was below a threshold necessary to induce CD8$^+$ T cell
177 proliferation **(Figure 1B)**. However, the addition of CD43 1B11 mAb agonism elicited robust
178 proliferation of CD8$^+$ T cells **(Figure 1B)**. These data demonstrate that the CD43 1B11 pathway
179 can provide a costimulatory signal to CD8$^+$ T cells when a sub-threshold strength of antigen
180 stimulation is present.
181

182 **3.2 CD43 mAb treatment overcomes tolerance to induce graft rejection.**

183 We reasoned that because CD43 1B11 can provide activating signals to CD8$^+$ T cells
184 and CD43 1B11$^+$ CD8$^+$ T cells are potent effectors, that signaling through this receptor could
185 elicit graft rejection. We induced tolerance with combined CD28/CD40 costimulation blockade
186 (CTLA-4 Ig and CD40L mAb; **Figure 1C**), and treated mice with CD43 1B11 mAb on day 8-14,
187 which corresponds to the initial expression of CD43 1B11 epitope on CD8$^+$ T cells [29]. We found
188 that while costimulation blockade induced graft survival to 30 days, treatment with CD43 1B11
189 elicited graft rejection in 63% of mice by day 20 **(Figure 1D)**. While costimulation blockade
190 elicited few activated effector CD8$^+$ T cells, mice treated with CD43 1B11 had a higher frequency
191 of CD62L^{lo}CD27^{lo} T cell population **(Figure 1E)**. This population is highly proliferative, as
192 denoted by expression of Ki67 **(Figure 1F)**. Together, these data demonstrate that activation of

193 the CD43 1B11 signaling pathway is critical for acute rejection, and can overcome
194 transplantation tolerance.
195
196 **3.3 The CD43$^+$ICOS$^+$ phenotype specifically identifies proliferative graft-specific CD8$^+$ T**
197 **cells**
198 As transplantation elicits relatively weak expansion of graft-specific CD8$^+$ T cells,[29,36] we
199 next evaluated whether the CD43 1B11$^+$ICOS$^+$ phenotype can be used to identify relatively rare
200 proliferative CD8$^+$ T cells after transplantation by evaluating expression of Ki67, which denotes
201 recently divided or actively proliferating T cells in H-2^b C57Bl/6 mice that received an H-2^d
202 Balb/c skin graft on day 14 post-grafting **(Figure 2A)**.
203 Among the canonical activation markers CD44^{hi} or CD62L^{lo}, many CD44^{hi} or CD62L^{lo}
204 cells were Ki67$^-$, indicating that these markers are highly sensitive, but not specific, for
205 proliferative graft-specific CD8$^+$ T cells **(Figure 2B)**. As previously published, we found that very
206 few KLRG-1$^+$ cells were elicited during acute rejection **(Figure 2B)**, precluding further analysis
207 of KLRG-1$^+$Ki67$^+$ cells. We found that 57.9±4.7% and 32±4.3% of CXCR3$^+$ cells were Ki67$^+$ in
208 the L^d QL9$^+$ and bulk CD8$^+$ T cell compartments, respectively **(Figure 2B)**. However, both CD43
209 1B11$^+$ and ICOS$^+$ populations were highly enriched for Ki67$^+$ CD8$^+$ T cells **(Figure 2B)**. Among
210 ICOS$^+$, 81.1±4.1% of L^d QL9$^+$ and 66.0±3.8% of bulk CD8$^+$ T cells were Ki67$^+$; among CD43
211 1B11$^+$ cells, 87.5±2.9% L^d QL9$^+$ and 64.5±4.7% bulk CD8$^+$ T cells were Ki67$^+$.
212 To directly visualize the proliferation of CD8$^+$ T cells during acute rejection, we adoptively
213 transferred polyclonal CellTrace Violet (CTV) labeled naïve CD45.1 CD8$^+$ T cells naïve C57Bl/6
214 (CD45.2) hosts, followed by Balb/c skin grafting **(Figure 2C)**. In parallel, we transferred CTV
215 labeled Thy1.1$^+$ OT-I CD8$^+$ T cells into C57Bl/6 hosts and provided Act-mOVA skin grafts as a
216 comparison high-affinity antigen-specific response. After 14 days, we identified the graft-specific
217 L^d QL9$^+$ CD8$^+$ T cells, bulk CD8$^+$ T cells, or OT-I cells using magnetic column enrichment.

218 Expression of ICOS and CD43 1B11 were largely restricted to divided cells in each population
219 **(Figure 2D-E)**. Among divided bulk $CD8^+$ T cells, the frequency of $ICOS^+$ cells was 41.6±4.9%,
220 while 73.6±4.8% were CD43 $1B11^+$. L^d $QL9^+$ $CD8^+$ T cells displayed a similar profile, with
221 divided cells being 84.2±7.5% $ICOS^+$ and 91.8±4.6% CD43 $1B11^+$. Thus, at this timepoint, while
222 both ICOS and CD43 1B11 are specific for proliferating $CD8^+$ T cells, CD43 1B11 is a slightly
223 more sensitive marker for proliferating graft-specific $CD8^+$ T cells.
224
225 **3.4 CD43 $1B11^+$ CD8+ T cells rapidly infiltrate heart allografts during acute rejection**
226 We evaluated whether the functional potency of CD43 $1B11^+$ $CD8^+$ T cells identified in
227 the secondary lymphoid organs corresponded to infiltration into fully vascularized heart
228 allografts during acute rejection. In this fully allogeneic heart graft model, acute rejection occurs
229 within 1 week post-graft [37,38]. We evaluated the phenotype of heart graft-infiltrating $CD8^+$ T cells
230 relative to the spleen on day 5 post-graft **(Figure 2G)**, and found that while only 7.4±3.6% of
231 $CD8^+$ T cells were CD43 $1B11^+$ $ICOS^+$ in the spleen at this early timepoint, 53.4±14.7% of graft
232 infiltrating $CD8^+$ T cells were CD43 $1B11^+ICOS^+$ **(Figure 2H)**. These data demonstrate that
233 CD43 $1B11^+$ $ICOS^+$ are a significant portion of the graft-infiltrating $CD8^+$ T cells during acute
234 rejection.
235
236 **3.5 CD43 $1B11^+$ $CD8^+$ T cells maintain expression of IL-7Rα and TCF1 during acute**
237 **rejection**
238 We next evaluated the expression of key effector and stem-like markers of graft-specific
239 $CD44^{hi}$ $CD8^+$ T cells at effector and memory timepoints **(Figure 3A)**. CD43 $1B11^+$ $CD8^+$ T cells
240 were nearly universally positive for Ki67 **(Figure 3B-C).** However, CD43 $1B11^+$ $CD8^+$ T cells also
241 expressed similarly high levels of IL-7Rα to naïve, $CD62L^{hi}$ and $CD62L^{lo}$ effector populations
242 **(Figure 3B-C)**. CD43 $1B11^+$ effectors expressed significantly higher levels of T-bet than either

243 CD43 1B11$^-$ effector population (85±2.9% CD43 1B11$^+$ vs 48±3.1% CD62L$^+$CD43 1B11$^-$ and
244 52±5.1% CD62L$^-$CD43 1B11$^+$; **Figure 3B-C**). Finally, CD43 1B11$^+$ CD8$^+$ T cells also maintained
245 relatively high levels of TCF-1 (69.9 ± 4.3%) similar to naïve and CD43 1B11$^-$ effector CD8$^+$ T
246 cell populations (**Figure 3B-C**). A similar expression profile of Ki67, IL-7Rα, T-bet, and TCF-1
247 was observed for bulk CD44^{hi} CD8$^+$ T cell populations **(Figure S1A-B)**.
248 At memory timepoint (>35 days post-graft), we found that all three populations of CD8$^+$ T
249 cells were high for IL-7Rα and TCF-1 **(Figure 3D-E)**. However, CD43 1B11$^+$ CD8$^+$ T cells
250 maintained higher expression of T-bet (72.6±3.9% CD43 1B11$^+$ vs 48.0±5.0% CD62L$^+$CD43
251 1B11$^-$ and 47.2±6.2% CD62L$^-$CD43 1B11$^+$; **Figure 3D-E**). Together, these data demonstrate that
252 CD43 1B11$^+$ CD8$^+$ T cells have an effector and memory program characterized by high T-bet
253 expression versus CD43 1B11$^-$ populations, but also largely maintain expression of stemness
254 markers IL-7Rα and TCF-1.
255
256 **3.6 Effector CD43 1B11 CD8$^+$ T cells persist relative to CD43 1B11$^-$ CD8$^+$ T cells after**
257 **transplantation**
258 We used an adoptive transfer approach to assess the fate, and potential persistence, of
259 CD43 1B11$^+$ CD8$^+$ T cells relative to CD43 1B11$^-$ CD8$^+$ T cells. We isolated CD62L^{lo} CD43 1B11$^-$
260 and CD43 1B11$^+$ CD8$^+$ T cells from CD45.1 recipients of Balb/c skin grafts using flow cytometric
261 sorting **(Figure 4A**). We adoptively transferred equal numbers of these cells into CD45.2
262 C57Bl/6 mice, challenged them with a Balb/c skin graft, and evaluated the number and
263 phenotype of transferred populations on day 21 post-graft.
264 We found that relative to CD43 1B11$^-$ T cells, greater numbers of CD43 1B11$^+$ T cells
265 were recovered from secondary lymphoid tissue **(Figure 4B)**. While CD43 1B11$^+$ T cells
266 remained CD43 1B11$^+$ after skin grafting, a fraction of CD43 1B11$^-$ T cells converted to CD43
267 1B11$^+$ T cells following the second skin graft challenge **(Figure 4C)**. Evaluation of the

268 localization of these transferred populations in the draining lymph node revealed that CD43
269 1B11^{+} population localizes to the high endothelial venule relative to the CD43 1B11^{-} CD8^{+} T
270 cells **(Figure 4D)**. Together, these data demonstrate that CD43 1B11^{+} CD8+ T cells appear to
271 be a terminal phenotype, as they are formed from CD43 1B11^{-} precursors, and are persistent *in*
272 *vivo*.
273
274 **3.7 CD8^{+} T cells that are *SPN*$^{+}$*GCNT1*$^{+}$ are present in the rejecting allografts of kidney**
275 **transplant patients experiencing acute rejection**
276 In order to investigate whether a population of CD43^{+} CD8^{+} T cells could be identified in
277 the allografts of kidney transplant patients during acute rejection, we explored the single cell
278 RNA-sequencing data generated by Shi et al [33] **(Figure 5A).** Among kidney transplant patients
279 undergoing acute cellular rejection, we identified 8 clusters of CD8^{+} T cells **(Figure 5B-C)**. All
280 clusters expressed the CD43 gene *SPN*. The because the glycosyltransferase GCNT1 is
281 responsible for glycosylating the CD43 receptor [13,27,28], we reasoned that *SPN*$^{+}$*GCNT1*$^{+}$ clusters
282 could be a surrogate for CD43 1B11^{+} CD8^{+} T cells observed using flow cytometry. We found that
283 clusters 1, 2, 4, and 6 were *SPN*$^{+}$*GCNT1*$^{+}$ **(Figure 5D)**. The *SPN*$^{+}$*GCNT1*$^{+}$ clusters were higher
284 for Granzyme B (*GZB*) and lower for CD62L (*SELL*), which is consistent with the CD43 1B11^{+}
285 CD8^{+} T cell population in mice. The *SPN*$^{+}$*GCNT1*$^{+}$ clusters expressed high levels of granzymes
286 and perforin (*GZMA, GZMH, GZMK, PRF1*). Relative to GCNT1^{-} clusters present in the allograft,
287 they expressed elevated transcripts for IFN-γ (*IFNG*), the chemokine receptor CXCR3, and the
288 co-receptors PD-1 and ICOS, which are markers of recent antigen encounter. Overall, these
289 results reveal that populations of CD8^{+} T cells that are *SPN*$^{+}$*GCNT1*$^{+}$ are present in rejecting
290 kidney allografts, and these clusters have features of highly potent effectors that have recently
291 encountered antigen.
292

293 **3.8 CD43 1D4 mAb identifies a population of effector CD8$^+$ T in healthy human donors**
294 **and kidney transplant candidates**

295 In humans, high and low molecular weight forms of the CD43 receptor have been
296 identified [39]. The CD43 1D4 mAb clone identifies a large core-2 O-glycosylated isoform of CD43
297 on human T cells [39]. In healthy donors, we found that a fraction of CD14$^+$ monocytes and CD8$^+$
298 T cells stained for CD43 1D4 **(Figure 6A)**. We investigated whether the CD43 1D4$^+$ CD8$^+$ T
299 cells corresponded with the canonical naïve (CCR7$^+$CD45RA^{hi}) or antigen-experienced T cell
300 populations: central memory (T_{CM}, CCR7$^+$CD45RA^{lo}), effector memory (T_{EM}, CCR7$^-$CD45RA^{lo}),
301 or T effector memory RA$^+$ (T_{EMRA}, CCR7$^-$CD45RA$^+$) populations. While CD43 ID4$^-$ CD8$^+$ T cells
302 were predominantly found within the naïve compartment, CD43 1D4$^+$ CD8$^+$ T cells were found
303 predominantly within antigen-experience fractions **(Figure 6B).** Further exploration of the
304 phenotype of these cells revealed that CD43 1D4$^+$ CD8$^+$ T cells had lower expression of CD27
305 and higher expression of CXCR3 and ICOS than CD43 1D4$^+$ CD8$^+$ T cells **(Figure 6C)**.

306 We next investigated whether CD43 1D4 was expressed on CD8$^+$ T cells from patients
307 with end-stage renal disease who are waitlisted for kidney transplantation. Similar to healthy
308 donors, a population of CD8$^+$ T cells expressed CD43 1D4 **(Figure 6D)**. We found that relative
309 to CD43 1D4$^-$, CD43 1D4$^+$ CD8$^+$ T cells had variable and statistically similar expression of
310 CD45RA and CCR7, demonstrating that this population did not correspond to a canonical T_{EM},
311 T_{CM}, or T_{EMRA} populations **(Figure 6E).** CD43 1D4$^+$ CD8$^+$ T cells from these patients also
312 displayed lower expression of CD27 and higher expression of ICOS and CXCR3 **(Figure 6F).**
313 Overall, these data demonstrate that CD43 1D4 identifies a population of antigen-experienced
314 CD8$^+$ T cells in human healthy donors and renal transplant candidates.
315

316 **3.9 CD43 1D4$^+$ CD8$^+$ T cells are efficient cytokine producers relative to CD43 1D4$^-$ CD8$^+$ T**
317 **cells**

318 To evaluate the functional capacity of CD43 1D4^{+} and CD43 1D4^{-} CD8^{+} T cells, we
319 stimulated PBMC from healthy donors with CD3ε mAb for 18-20 hours and evaluated CD8^{+} T
320 cells based on CD45RA and CD43 1D4 expression **(Figure S2A and Figure 6G).** We found that
321 CD3ε mAb stimulation increased CD43 1D4 expression among both CD45RA^{hi} and CD45RA^{lo}
322 populations **(Figure S2B)**. This change was very modest among CD45RA^{lo} cells, and was more
323 pronounced among CD45RA^{hi} cells, presumably due to activation of a subset of naïve CD8^{+} T
324 cells. When we compared the cytokine production among CD43 1D4^{+} and 1D4^{-} fractions, we
325 found that both CD45RA^{hi} and CD45RA^{lo} CD43 1D4^{+} fractions produced elevated levels of TNF-
326 α and IFN-γ relative to the CD43 1D4^{-} populations **(Figure 6D).** In total, these data demonstrate
327 that CD43 1D4 is a marker of antigen-experienced and acute effector CD8^{+} cells that are
328 functional as determined by cytokine production.
329
330
331

332 **4. DISCUSSION**

333

334 In this study, we built upon previous work that showed graft-specific L^d $QL9^+$ $CD8^+$ T
335 cells express the activated glycoform of the siaolomucin CD43, defined by the 1B11 mAb.[29]
336 Specifically, we sought to evaluate whether CD43 1B11 a marker of short-lived, highly
337 proliferative $CD8^+$ T cells, analogous to KLRG-1^+ short-lived effector $CD8^+$ T cells.
338 We found that treatment with CD43 1B11 mAb *in vivo* was able to break costimulation-
339 blockade induced tolerance and elicit skin graft rejection in the majority of mice after Balb/c skin
340 grafting. To our knowledge, prior studies using CD43 mAb have not distinguished between
341 global signaling through the CD43 receptor and the specific function of activated CD43 $1B11^+$
342 receptor.[25,34,35] Our results demonstrate that CD43 1B11 agonism provides a costimulatory
343 signal to $CD8^+$ T cells that can overcome sub-threshold antigen signaling, and that this pathway
344 is critical for alloimmunity *in vivo*.
345 We found that CD43 $1B11^+$ status was highly sensitive for proliferating $CD8^+$ T cells
346 during acute rejection, and that CD43 $1B11^+$ $CD8^+$ T cells are a significant fraction of graft-
347 infiltrating $CD8^+$ T cells during acute rejection of heart allografts. Consistent with a highly potent
348 effector phenotype, CD43 $1B11^+$ $CD8^+$ T cells had higher levels of T-bet expression versus
349 CD43 $1B11^-$ $CD8^+$ T cell populations. However, in contrast to terminally differentiated effector
350 $CD8^+$ T cells, CD43 $1B11^+$ $CD8^+$ T cells also maintained expression of memory-precursor and
351 stem-like makers TCF-1 and IL-7Rα, and were more persistent in adoptive transfer
352 experiments. TCF1 is associated with the survival and proliferative capacity of T cells in a
353 variety of settings,[18,19,43,44] and TCF1 expression in $CD4^+$ T cells corresponds with self-renewal
354 capacity of effectors in transplantation.[43] Further work is needed to understand the importance
355 of the heterogeneity of TCF-1 expression within the CD43 $1B11^+$ population, including whether
356 this population is predominantly self-renewing or fed by CD43 $1B11^-$ cells.

357 In total, these results demonstrate that CD43 1B11^{+} CD8^{+} T cells possess a combination
358 of effector and stem-like features: potent effector capacity (cytokine production, rapid graft
359 infiltration, localization near the HEV), robust proliferation, and enhanced survival. In contrast to
360 the early memory-effector precursor model after viral infection, our findings point to a
361 progressive differentiation model of CD8^{+} T cell activation in which CD43 1B11^{+} CD8^{+} T cells
362 dominate the proliferative cytotoxic response during the acute phase, but also efficiently persist
363 into memory after antigen clearance. Additional studies are needed to further dissect the
364 population dynamics of the CD43 1B11^{+} population and elucidate the full transcriptional program
365 driving its function. Future studies are needed to explore the potential approaches to
366 therapeutically target them in mice and humans.
367
368

ACKNOWLEDGEMENTS/FUNDING

We thank members of the Johns Hopkins Department of Pathology Division of Immunology for helpful discussions. We appreciate Hao Zhang and the Bloomberg School of Public Health Flow Cytometry and Cell Sorting Core for excellent cell sorting, the Johns Hopkins Ross Flow Cytometry Core, and the NIH Tetramer Core Facility for tetramer reagents and technical advice. We thank the Johns Hopkins Collaborative Outcomes Research in Endocrine Surgery (CORES) for human subject sample collection and storage. This work was supported by National Institute of Allergy and Infection Disease (NIAID) R56 AI179856 (S.M.K.), American Society of Transplantation Research Network Career Transition Grant (S.M.K.), KidneyCure Carl W. Gottschalk Research Scholar Grant (S.M.K.), NIAID R01 AI114496 (J.S.B.), National Heart, Lung, and Blood Institute (NLBI) R01HL118183 (D.C.), NHLBI R01HL136586 (D.C.), National Cancer Institute R01CA289729 (D.C.), The American Heart Association 23EIA1040103 (D.C.), Global Autoimmune Institute (D.C.), and the Matthew Poyner MVP Memorial Myocarditis Research Fund (D.C.).

DISCLOSURE

The authors declare no competing interests.

DATA AVAILABILITY STATEMENT

Further information and requests for resources and reagents should be directed to the lead contact, Scott Krummey (skrumme1@jhmi.edu)

AUTHOR CONTRIBUTIONS

Conceptualization, S.M.K., G.S.C., J.S.B., R.P.L., J.S.F., B.O., D.C.; methodology, G.S.C., J.S.F., M.W.S., R.H., S.M.K., C.M., J.S.B., R.W.; formal analysis, S.M.K., G.S.C., M.W.S.; investigation, G.S.C., J.S.F., R.P.L., M.W.S., R.H., R.W.; writing, G.S.C., S.M.K.; visualization, S.M.K., G.S.C., J.S.F., R.P.L.; supervision, S.M.K., J.S.B., C.M., D.C.

403 **FIGURE LEGENDS**

404

405 **Figure 1. Treatment with CD43 1B11 mAb can break costimulation-blockade induced**
406 **tolerance.** (A) C57Bl/6 mice were provided with Balb/c skin grafts and treated with tolerance-
407 inducing costimulation-blockade with CTLA-4 Ig and CD154 mAb (250 μg/dose, post-graft day 0,
408 2, 4, 6). Groups of mice were treated with IgG2a isotype control or CD43 1B11 mAb (200 μg/dose)
409 on post-graft day 8, 11, and 14. (B) On post-graft day 14, the phenotype of $CD8^+$ T cells was
410 assessed in the blood of skin grafted mice. (C) The expression of Ki67 was assessed on
411 populations of $CD8^+$ T cells in the blood from B. (D) Skin graft survival was assessed on mice
412 treated as described in A. Each data point depicts an individual mouse. Summary data depicts
413 pooled results from 2 independent experiments (n=6-8 mice/group) and depicts mean ± SEM.
414 Statistics performed by (B) Student's t-test (2-tailed), (C) (C) 1-way ANOVA or (E) mixed-effects
415 model (REML) with Tukey's multiple comparisons test or (E) unpaired Student's t-test. Error bars
416 depict SEM. **p<0.01, ***p<0.001, ****p<0.0001.

417

418 **Figure 2. Proliferative $CD8^+$ T cells are defined by CD43 $1B11^+$ and $ICOS^+$ phenotype after**
419 **transplantation.** (A) C57Bl/6 mice were provided with Balb/c skin grafts and $CD8^+$ T cells were
420 assessed on day post-graft 14 in the spleen and graft draining lymph nodes. (B) Representative
421 flow and summary data depicting the frequency of $Ki67^+$ cells among $CD8^+$ T cells expressing the
422 indicated marker. Minimal expression of KLRG-1 precluded analysis. (C) $2x10^6$ naïve CD45.1 or
423 $1x10^6$ Thy1.1 OT-I $CD8^+$ T cells labeled with CellTrace Violet were adoptively transferred into
424 CD45.2 C57Bl/6 mice, who were provided with Balb/c or Act-mOVA skin grafts, respectively.
425 Transferred cells were enriched using paramagnetic beads specific for APC, which stained with
426 Thy1.1 or L^d QL9 tetramers. (D) Among the adoptively transferred $CD8^+$ T cell populations, gates
427 were drawn around the undivided (gray) and proliferation (orange) populations. The minimal

428 number of undivided OT-I cells precluded further analysis. (E) The frequency of ICOS$^+$ cells
429 among each indicated adoptively transferred CD8$^+$ T cell population. (F) Frequency of CD43
430 1B11$^+$ cells among each indicated adoptively transferred CD8$^+$ T cell population. (G-H) C57Bl/6
431 mice were provided with heterotopic Balb/c heart grafts and the phenotype of CD8$^+$ T cells was
432 assessed in the spleen and heart graft on day 5 post-graft. Each data point depicts an individual
433 mouse. Summary data depicts pooled results from 2-5 independent experiments (n=5-10
434 mice/group) and depicts mean ± SEM. Statistics performed by (B) 1-way ANOVA with Dunnett's
435 multiple comparison test versus CD44^{hi} and (H) unpaired Student's t-test (2-tailed). Error bars
436 depict SEM. N.D, no data, due to low cell numbers. *p<0.05, **p<0.01, ***p<0.001, ****p<0.0001.
437
438 **Figure 3. Graft-specific CD43 1B11$^+$ CD8$^+$ T cells have both effector and stem-like**
439 **phenotypic features.** (A) C57Bl/6 mice were provided with Balb/c skin grafts and CD8$^+$ T cells
440 were assessed on day 14 post-graft (Acute Effector) or day >35 post-graft (Memory) in pooled
441 spleen and graft draining lymph nodes. Graft-specific cells were identified after enrichment using
442 L^d QL9 tetramers and APC microbeads, and gated based on CD62L and CD43 1B11 expression
443 as depicted. (B) Representative flow plots and (C) summary data depicting expression of Ki67,
444 IL-7Rα, TCF-1, and T-bet among CD44^{lo} or CD44^{hi} L^d QL9$^+$ CD8$^+$ T cell populations at the Acute
445 Effector timepoint. See also **Figure S1.** (D) Representative flow plots and (E) summary data
446 depicting expression of Ki67, IL-7Rα, TCF-1, and T-bet among CD44^{lo} or CD44^{hi} L^d QL9$^+$ CD8$^+$ T
447 cell populations at the Memory timepoint. Summary data depicts pooled results from 2-3
448 independent experiments (n=8-14 mice/group) and depicts mean ± SEM. Statistics performed by
449 (C, E) 1-way ANOVA with Tukey's multiple comparison test (excluding CD44^{lo} population used as
450 a staining control). Error bars depict SEM. *p<0.05, **p<0.01, ***p<0.001, ***p<0.0001.
451

452 **Figure 4. CD43 1B11$^+$ CD8$^+$ T cells are persistent after grafting relative to CD43 1B11$^-$ CD8$^+$**
453 **T cells.** (A) Effector CD45.1 CD8$^+$ T cells (post-graft day 10-14 after Balb/c skin grafts) were flow
454 cytometrically sorted into CD43 1B11$^+$ and CD43 1B11$^-$ populations. 1x10^5 were adoptively
455 transferred into C57Bl/6 (CD45.2) hosts, who were provided with Balb/c skin grafts the following
456 day. Transferred cells were assessed on post-graft day 14. (B) Recovery of CD43 1B11$^+$ and
457 CD43 1B11$^-$ CD8$^+$ T cells in the secondary lymphoid organs. (C) Frequency of CD43 1B11$^+$ CD8$^+$
458 T cells among adoptively transferred populations. (D) Immunofluorescence histology of draining
459 lymph nodes depicting adoptively transferred CD45.1 CD8$^+$ T cells (red) and the HEV marker ER-
460 TR7 (green). Arrows depict localization of adoptively transferred CD45.1 CD8$^+$ T cells outside
461 (CD43 1B11$^-$) or within (CD43 1B11$^+$) HEV. Summary data depicts pooled results from 3
462 independent experiments (n=6-10 mice/group) and depicts mean ± SEM. Statistics performed by
463 unpaired Student's t-test (2-tailed). Error bars depict SEM. HEV, high endothelial venule. *p<0.05,
464 **p<0.01, ***p<0.001, ***p<0.0001.
465
466 **Figure 5. A population of effector-like graft-infiltrating CD8$^+$ T cells from kidney transplant**
467 **patients are *SPN$^+$GCNT1$^+$*.** (A) Biopsies from kidney transplant patients with clinical signs of
468 acute rejection were analyzed by single cell RNA-sequencing. (B) Hierarchical clustering and U-
469 MAP analysis of CD8$^+$ T cells from kidney allograft biopsies. (C) Expression of *SPN, GCNT1,*
470 *GZMB,* and *SEL*L among CD8$^+$ T cell clusters. (D) Heatmap depicting expression genes for T cell
471 of co-receptor and effector proteins.
472
473 **Figure 6. A population of human CD8$^+$ T cells are CD43 1D4$^+$ and have an antigen-**
474 **experienced effector phenotype.** (A) The frequency of peripheral healthy donor CD14$^+$
475 monocytes and CD8$^+$ T cells that express the CD43 epitope 1D4. (B-C) Expression of CD45RA
476 and CCR7 among CD43 1D4$^+$ and 1D4$^-$ CD8$^+$ T cells from healthy donors. (C) Representative
477 flow plots and summary data showing expression of CD27, CXCR3, and ICOS among CD43 1D4$^+$

478 and 1D4$^-$ CD8$^+$ T cell populations. (D) Frequency of CD43 1D4$^+$ CD8$^+$ T cells among kidney
479 transplant candidates. (E) Expression of CD45RA, CCR7 among CD43 1D4$^+$ and CD43 1D4$^-$
480 CD8$^+$ T cells from kidney transplant candidates. (F) Expression of CD27, CXCR3, and ICOS,
481 among CD43 1D4$^+$ and CD43 1D4$^-$ CD8$^+$ T cells from kidney transplant candidates. (G) Healthy
482 donor PBMC were stimulated for 20-24 h with CD3ε mAb (OKT3) and assessed for TNF-α and
483 IFN-γ production. See also **Figure S2**. (H) Summary data depicting the proportion of TNF-α (left)
484 or IFN-γ (right) produced by each CD45RA and CD43 1D4 quadrant population. Each data point
485 depicts an individual human donor. Summary data depicts pooled results from (A-C) 3
486 independent experiments (n=12-13 individuals/group), (D-F) 2 independent experiments (n=10
487 individuals/group), (H) 3 independent experiments (n=11 individuals/group). Summary data and
488 depicts mean $\pm$ SEM. Statistics performed by (B) 2-way ANOVA with Sidak's multiple comparisons
489 test and (C, E) paired Student's t-test (2-tailed), (G) 1-way ANOVA with Dunnett's multiple
490 comparisons test. Error bars depict SEM. *p<0.05, **p<0.01, ***p<0.001, ****p<0.0001.
491
492 **Figure S1. CD43 1B11$^+$ CD8$^+$ T cells have both effector and stem-like phenotypic features.**
493 Related to **Figure 3.** C57Bl/6 mice were provided with Balb/c skin grafts and CD8$^+$ T cells were
494 assessed on day 14 post-graft (Acute Effector) in the pooled spleen and graft draining lymph
495 nodes. (A) Representative flow plots and (B) summary data depicting expression of Ki67, IL-7Rα,
496 TCF-1, and T-bet among CD44^{lo} or CD44^{hi} L^d QL9$^+$ CD8$^+$ T cell populations at the Acute Effector
497 timepoint. Summary data depicts pooled results from 2-3 independent experiments (n=8-14
498 mice/group) and depicts mean $\pm$ SEM. Statistics performed by 1-way ANOVA with Tukey's multiple
499 comparison test (excluding CD44^{lo} population used as staining control). Error bars depict SEM.
500 *p<0.05, **p<0.01, ***p<0.001, ***p<0.0001.
501

502 **Figure S2. Evaluation of cytokine production by human CD43 1D4^{+} CD8^{+} T cell populations**.
503 Related to **Figure 6**. (A) Healthy donor PBMC were stimulated for 20-24 h with CD3ε mAb (OKT3)
504 and assessed for TNF-α and IFN-γ production. (B) Representative flow cytometry plots and
505 summary data showing expression of CD43 1D4 expression among CD45RA^{hi} and CD45RA^{lo}
506 populations of CD8^{+} T cells. Summary data depicts pooled results from 3 independent
507 experiments (n=11 individuals/group), and depict mean ± SEM. Statistics performed by (B) paired
508 Student's t-test (2-tailed), **p<0.01, ****p<0.0001
509
510

SUPPLEMENTAL INFORMATION

Additional supporting information may be found online in the Supporting Information section.

516

517 **REFERENCES**

518

519 1. Callemeyn J, Lamarthée B, Koenig A, Koshy P, Thaunat O, Naesens M. Allorecognition
520 and the spectrum of kidney transplant rejection. *Kidney Int*. Published online December
521 2021. doi:10.1016/j.kint.2021.11.029

522 2. Cherukuri A, Salama AD, Mehta R, et al. Transitional B cell cytokines predict renal
523 allograft outcomes. *Sci Transl Med*. 2021;13(582). doi:10.1126/scitranslmed.abe4929

524 3. Cole EH, Johnston O, Rose CL, Gill JS. Impact of Acute Rejection and New-Onset
525 Diabetes on Long-Term Transplant Graft and Patient Survival. *Clinical Journal of the*
526 *American Society of Nephrology*. 2008;3(3). doi:10.2215/CJN.04681107

527 4. Zaitsu M, Issa F, Hester J, Vanhove B, Wood KJ. Selective blockade of CD28 on human
528 T cells facilitates regulation of alloimmune responses. *JCI Insight*. 2017;2(19).
529 doi:10.1172/jci.insight.89381

530 5. Liu D, Badell IR, Ford ML. Selective CD28 blockade attenuates CTLA-4–dependent
531 CD8+ memory T cell effector function and prolongs graft survival. *JCI Insight*. 2018;3(1).
532 doi:10.1172/jci.insight.96378

533 6. Crepeau RL, Ford ML. Challenges and opportunities in targeting the CD28/CTLA-4
534 pathway in transplantation and autoimmunity. *Expert Opin Biol Ther*. 2017;17(8):1001-
535 1012. doi:10.1080/14712598.2017.1333595

536 7. Ford ML, Adams AB, Pearson TC. Targeting co-stimulatory pathways: transplantation and
537 autoimmunity. *Nat Rev Nephrol*. 2014;10(1):14-24. doi:10.1038/nrneph.2013.183

538 8. Krummey SM, Ford ML. Heterogeneity within T Cell Memory: Implications for Transplant
539 Tolerance. *Front Immunol*. 2012;3. doi:10.3389/fimmu.2012.00036

540 9. Jameson SC, Masopust D. Understanding Subset Diversity in T Cell Memory. *Immunity*.
541 2018;48(2):214-226. doi:10.1016/j.immuni.2018.02.010

542 10. Chung HK, McDonald B, Kaech SM. The architectural design of CD8+ T cell responses in
543 acute and chronic infection: Parallel structures with divergent fates. *Journal of*
544 *Experimental Medicine*. 2021;218(4). doi:10.1084/jem.20201730

545 11. Ford ML. T Cell Cosignaling Molecules in Transplantation. *Immunity*. 2016;44(5).
546 doi:10.1016/j.immuni.2016.04.012

547 12. Zehn D, Thimme R, Lugli E, de Almeida GP, Oxenius A. 'Stem-like' precursors are the
548 fount to sustain persistent CD8+ T cell responses. *Nat Immunol*. 2022;23(6):836-847.
549 doi:10.1038/s41590-022-01219-w

550 13. Nolz JC. Molecular mechanisms of CD8+ T cell trafficking and localization. *Cellular and*
551 *Molecular Life Sciences*. 2015;72(13):2461-2473. doi:10.1007/s00018-015-1835-0

552 14. Zehn D, Lee SY, Bevan MJ. Complete but curtailed T-cell response to very low-affinity
553 antigen. *Nature*. 2009;458(7235):211-214. doi:10.1038/nature07657

554 15. King CG, Koehli S, Hausmann B, Schmaler M, Zehn D, Palmer E. T Cell Affinity
555 Regulates Asymmetric Division, Effector Cell Differentiation, and Tissue Pathology.
556 *Immunity*. 2012;37(4):709-720. doi:10.1016/j.immuni.2012.06.021

557 16. Joshi NS, Cui W, Chandele A, et al. Inflammation Directs Memory Precursor and Short-
558 Lived Effector CD8+ T Cell Fates via the Graded Expression of T-bet Transcription
559 Factor. *Immunity*. 2007;27(2). doi:10.1016/j.immuni.2007.07.010

560 17. Kaech SM, Cui W. Transcriptional control of effector and memory CD8+ T cell
561 differentiation. *Nat Rev Immunol*. 2012;12(11):749-761. doi:10.1038/nri3307

562 18. Broomfield BJ, Groom JR. Defining the niche for stem-like CD8+ T cell formation and
563 function. *Curr Opin Immunol*. 2024;89:102454. doi:10.1016/j.coi.2024.102454

564 19. Im SJ, Obeng RC, Nasti TH, et al. Characteristics and anatomic location of PD-1 $^{+}$ TCF1 $^{+}$
565 stem-like CD8 T cells in chronic viral infection and cancer. *Proceedings of the National*
566 *Academy of Sciences*. 2023;120(41). doi:10.1073/pnas.2221985120

567 20. Im SJ, Hashimoto M, Gerner MY, et al. Defining CD8+ T cells that provide the proliferative
568 burst after PD-1 therapy. *Nature*. 2016;537(7620):417-421. doi:10.1038/nature19330

569 21. Braza F, Brouard S, Chadban S, Goldstein DR. Role of TLRs and DAMPs in allograft
570 inflammation and transplant outcomes. *Nat Rev Nephrol*. 2016;12(5):281-290.
571 doi:10.1038/nrneph.2016.41

572 22. Colvin MM, Smith CA, Tullius SG, Goldstein DR. Aging and the immune response to
573 organ transplantation. *Journal of Clinical Investigation*. 2017;127(7):2523-2529.
574 doi:10.1172/JCI90601

575 23. Onami TM, Harrington LE, Williams MA, et al. Dynamic Regulation of T Cell Immunity by
576 CD43. *The Journal of Immunology*. 2002;168(12):6022-6031.
577 doi:10.4049/jimmunol.168.12.6022

578 24. Mody PD, Cannon JL, Bandukwala HS, et al. Signaling through CD43 regulates CD4 T-
579 cell trafficking. *Blood*. 2007;110(8):2974-2982. doi:10.1182/blood-2007-01-065276

580 25. Sperling AI, Green JM, Mosley RL, et al. CD43 is a murine T cell costimulatory receptor
581 that functions independently of CD28. *Journal of Experimental Medicine*.
582 1995;182(1):139-146. doi:10.1084/jem.182.1.139

583 26. Clark MC, Baum LG. T cells modulate glycans on CD43 and CD45 during development
584 and activation, signal regulation, and survival. *Ann N Y Acad Sci*. 2012;1253(1):58-67.
585 doi:10.1111/j.1749-6632.2011.06304.x

586 27. Perkey E, Maurice De Sousa D, Carrington L, et al. GCNT1-Mediated O-Glycosylation of
587 the Sialomucin CD43 Is a Sensitive Indicator of Notch Signaling in Activated T Cells. *J*
588 *Immunol*. 2020;204(6):1674-1688. doi:10.4049/jimmunol.1901194

589 28. Nolz JC, Harty JT. IL-15 regulates memory CD8+ T cell O-glycan synthesis and affects
590 trafficking. *Journal of Clinical Investigation*. 2014;124(3):1013-1026.
591 doi:10.1172/JCI72039

592 29. Cohen GS, Kallarakal MA, Jayaraman S, et al. Transplantation elicits a clonally diverse
593 CD8+ T cell response that is comprised of potent CD43+ effectors. *Cell Rep*.
594 2023;42(8):112993. doi:10.1016/j.celrep.2023.112993

595 30. Hikono H, Kohlmeier JE, Takamura S, Wittmer ST, Roberts AD, Woodland DL. Activation
596 phenotype, rather than central– or effector–memory phenotype, predicts the recall
597 efficacy of memory CD8+ T cells. *Journal of Experimental Medicine*. 2007;204(7):1625-
598 1636. doi:10.1084/jem.20070322

599 31. Trambley J, Bingaman AW, Lin A, et al. Asialo GM1+ CD8+ T cells play a critical role in
600 costimulation blockade–resistant allograft rejection. *Journal of Clinical Investigation*.
601 1999;104(12):1715-1722. doi:10.1172/JCI8082

602 32. Liu F, Kang SM. Heterotopic Heart Transplantation in Mice. *Journal of Visualized*
603 *Experiments*. 2007;(6). doi:10.3791/238

604 33. Shi T, Burg AR, Caldwell JT, et al. Single-cell transcriptomic analysis of renal allograft
605 rejection reveals insights into intragraft TCR clonality. *J Clin Invest*. 2023;133(14).
606 doi:10.1172/JCI170191

607 34. Walker J, Green JM. Structural requirements for CD43 function. *J Immunol*.
608 1999;162(7):4109-4114.

609 35. Manjunath N, Correa M, Ardman M, Ardman B. Negative regulation of T-cell adhesion
610 and activation by CD43. *Nature*. 1995;377(6549):535-538. doi:10.1038/377535a0

611 36. Bozeman AM, Laurie SJ, Haridas D, Wagener ME, Ford ML. Transplantation
612 preferentially induces a KLRG-1lo CD127hi differentiation program in antigen-specific
613 CD8+ T cells. *Transpl Immunol*. 2018;50. doi:10.1016/j.trim.2018.06.003

614 37. Young JS, Khiew SHW, Yang J, et al. Successful Treatment of T Cell-Mediated Acute
615 Rejection with Delayed CTLA4-Ig in Mice. *Front Immunol*. 2017;8.
616 doi:10.3389/fimmu.2017.01169

617 38. Schwarz C, Unger L, Mahr B, et al. The Immunosuppressive Effect of CTLA4
618 Immunoglobulin Is Dependent on Regulatory T Cells at Low But Not High Doses.
619 *American Journal of Transplantation*. 2016;16(12):3404-3415. doi:10.1111/ajt.13872

620 39. Mukasa R, Homma T, Ohtsuki T, et al. Core 2-containing O-glycans on CD43 are
621 preferentially expressed in the memory subset of human CD4 T cells. *Int Immunol*.
622 1999;11(2):259-268. doi:10.1093/intimm/11.2.259

623 40. Ford ML, Onami TM, Sperling AI, Ahmed R, Evavold BD. CD43 Modulates Severity and
624 Onset of Experimental Autoimmune Encephalomyelitis. *The Journal of Immunology*.
625 2003;171(12):6527-6533. doi:10.4049/jimmunol.171.12.6527

626 41. Fay KT, Chihade DB, Chen CW, et al. Increased mortality in CD43-deficient mice during
627 sepsis. *PLoS One*. 2018;13(9):e0202656. doi:10.1371/journal.pone.0202656

628 42. Ford ML, Evavold BD. Modulation of MOG 37–50-specific CD8+ T cell activation and
629 expansion by CD43. *Cell Immunol*. 2006;240(1):53-61.
630 doi:10.1016/j.cellimm.2006.06.007

631 43. Zou D, Yin Z, Yi SG, et al. CD4+ T cell immunity is dependent on an intrinsic stem-like
632 program. *Nat Immunol*. 2024;25(1):66-76. doi:10.1038/s41590-023-01682-z

633 44. Mo F, Yu Z, Li P, et al. An engineered IL-2 partial agonist promotes CD8+ T cell
634 stemness. *Nature*. 2021;597(7877):544-548. doi:10.1038/s41586-021-03861-0

635 45. Duckworth BC, Lafouresse F, Wimmer VC, et al. Effector and stem-like memory cell fates
636 are imprinted in distinct lymph node niches directed by CXCR3 ligands. *Nat Immunol*.
637 2021;22(4):434-448. doi:10.1038/s41590-021-00878-5

638

639

Figure 1

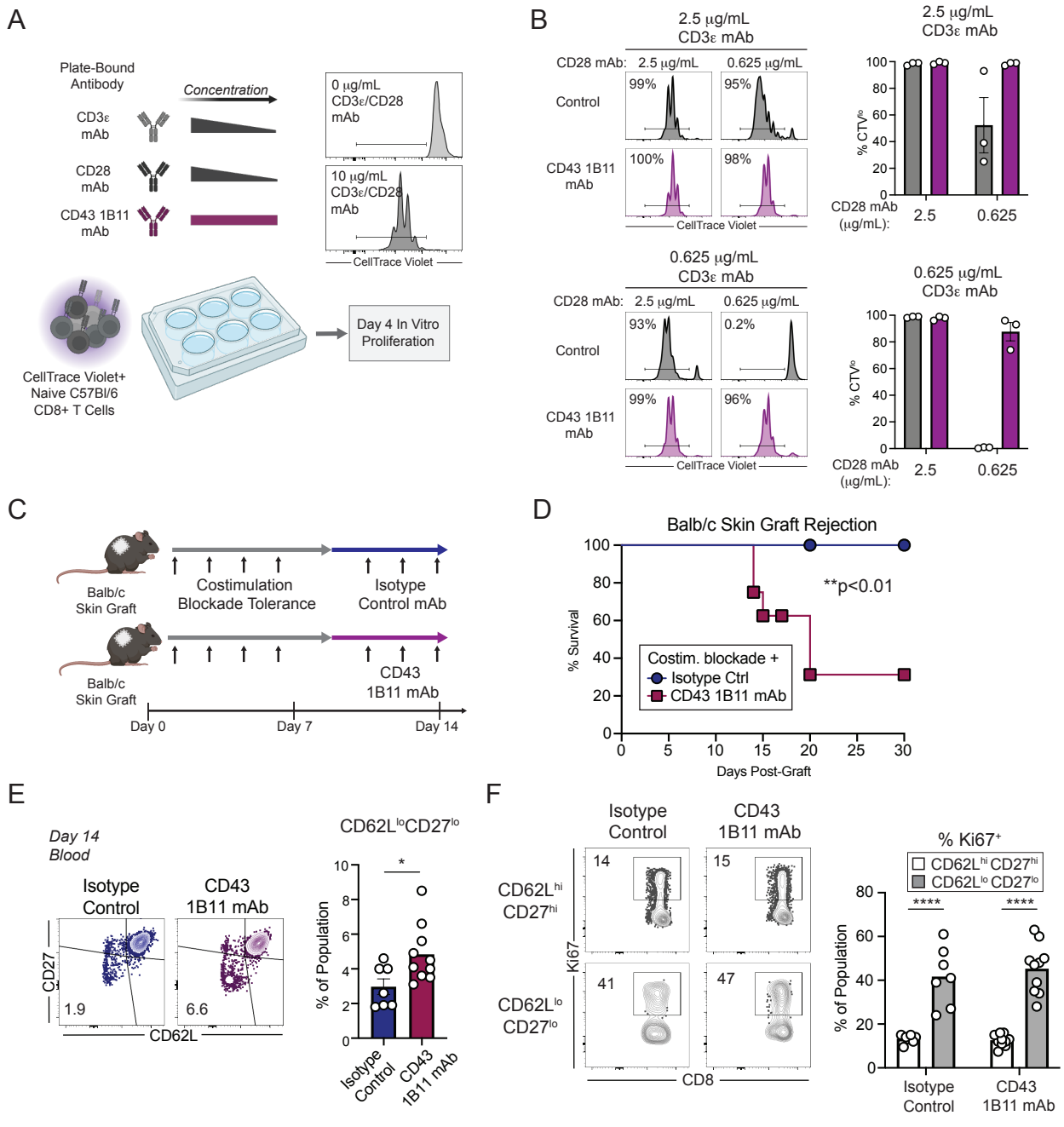
A
Plate-Bound Antibody
Concentration
CD3ε mAb
CD28 mAb
CD43 1B11 mAb
0 μg/mL CD3ε/CD28 mAb
10 μg/mL CD3ε/CD28 mAb
CellTrace Violet
CellTrace Violet+ Naive C57Bl/6 CD8+ T Cells
Day 4 In Vitro Proliferation
B
2.5 μg/mL CD3ε mAb
CD28 mAb: 2.5 μg/mL 0.625 μg/mL
Control
CD43 1B11 mAb
99%
95%
100%
98%
CellTrace Violet
% CTV^lo
CD28 mAb (μg/mL): 2.5 0.625
0.625 μg/mL CD3ε mAb
93%
0.2%
99%
96%
C
Balb/c Skin Graft
Costimulation Blockade Tolerance
Isotype Control mAb
CD43 1B11 mAb
Day 0
Day 7
Day 14
D
Balb/c Skin Graft Rejection
% Survival
**p<0.01
Costim. blockade +
Isotype Ctrl
CD43 1B11 mAb
Days Post-Graft
E
Day 14 Blood
Isotype Control
CD43 1B11 mAb
CD27
CD62L
1.9
6.6
CD62L^lo CD27^lo
% of Population
Isotype Control
CD43 1B11 mAb
F
Isotype Control
CD43 1B11 mAb
CD62L^hi CD27^hi
CD62L^lo CD27^lo
Ki67
CD8
14
15
41
47
% Ki67^+
CD62L^hi CD27^hi
CD62L^lo CD27^lo
****
% of Population
Isotype Control
CD43 1B11 mAb

Figure 2

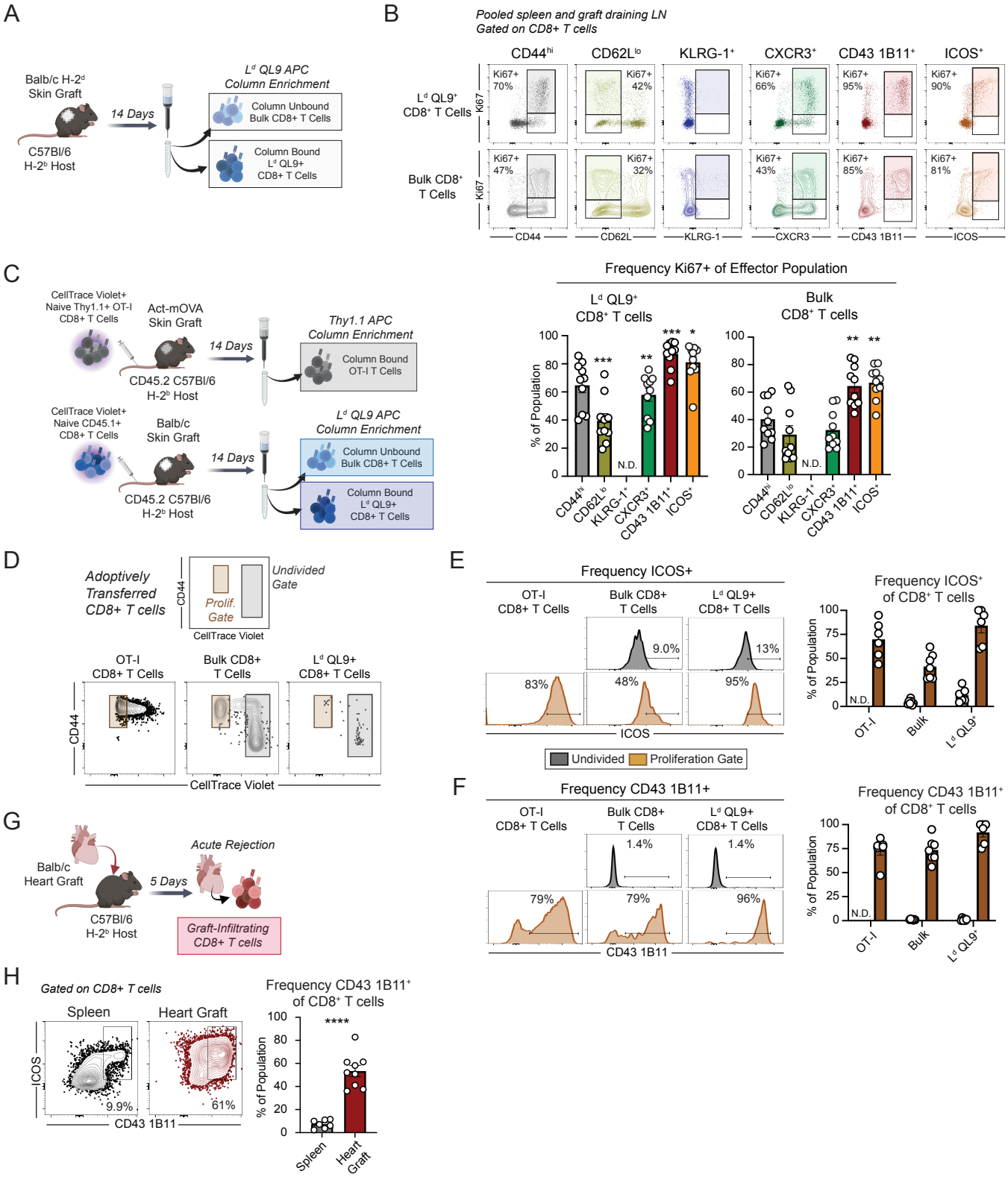
A
Balb/c H-2d Skin Graft
C57Bl/6 H-2b Host
14 Days
Ld QL9 APC Column Enrichment
Column Unbound Bulk CD8+ T Cells
Column Bound Ld QL9+ CD8+ T Cells
B
Pooled spleen and graft draining LN
Gated on CD8+ T cells
CD44hi
CD62Llo
KLRG-1+
CXCR3+
CD43 1B11+
ICOS+
Ld QL9+ CD8+ T Cells
Bulk CD8+ T Cells
Ki67
Ki67+ 70%
Ki67+ 42%
Ki67+ 66%
Ki67+ 95%
Ki67+ 90%
Ki67+ 47%
Ki67+ 32%
Ki67+ 43%
Ki67+ 85%
Ki67+ 81%
C
CellTrace Violet+ Naive Thy1.1+ OT-I CD8+ T Cells
Act-mOVA Skin Graft
CD45.2 C57Bl/6 H-2b Host
Thy1.1 APC Column Enrichment
Column Bound OT-I T Cells
CellTrace Violet+ Naive CD45.1+ CD8+ T Cells
Balb/c Skin Graft
Frequency Ki67+ of Effector Population
% of Population
N.D.
D
Adoptively Transferred CD8+ T cells
Undivided Gate
Prolif. Gate
CD44
CellTrace Violet
OT-I CD8+ T Cells
Bulk CD8+ T Cells
Ld QL9+ CD8+ T Cells
E
Frequency ICOS+
9.0%
13%
83%
48%
95%
ICOS
Undivided
Proliferation Gate
Frequency ICOS+ of CD8+ T cells
F
Frequency CD43 1B11+
1.4%
1.4%
79%
79%
96%
CD43 1B11
Frequency CD43 1B11+ of CD8+ T cells
G
Balb/c Heart Graft
C57Bl/6 H-2b Host
5 Days
Acute Rejection
Graft-Infiltrating CD8+ T cells
H
Gated on CD8+ T cells
Spleen
Heart Graft
9.9%
61%
Frequency CD43 1B11+ of CD8+ T cells
Spleen
Heart Graft

Figure 3

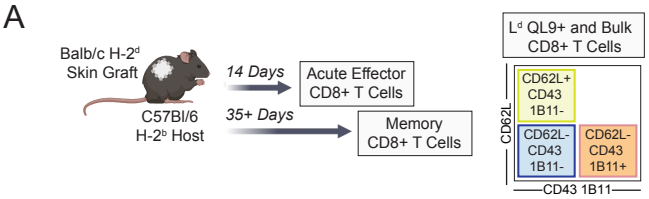
A
Balb/c H-2d
Skin Graft
C57Bl/6
H-2b Host
14 Days
Acute Effector
CD8+ T Cells
35+ Days
Memory
CD8+ T Cells
Ld QL9+ and Bulk
CD8+ T Cells
CD62L+
CD43
1B11-
CD62L-
CD43
1B11-
CD62L-
CD43
1B11+
CD62L
CD43 1B11

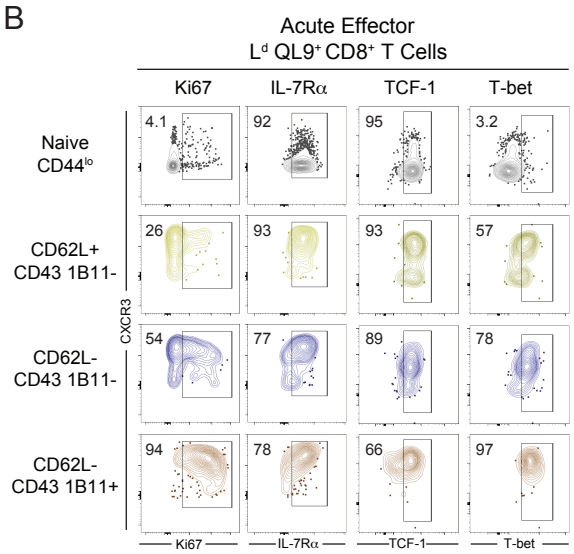
B
Acute Effector
Ld QL9+ CD8+ T Cells
Ki67
IL-7Rα
TCF-1
T-bet
Naive
CD44lo
CD62L+
CD43 1B11-
CD62L-
CD43 1B11-
CD62L-
CD43 1B11+
CXCR3
4.1
92
95
3.2
26
93
93
57
54
77
89
78
94
78
66
97

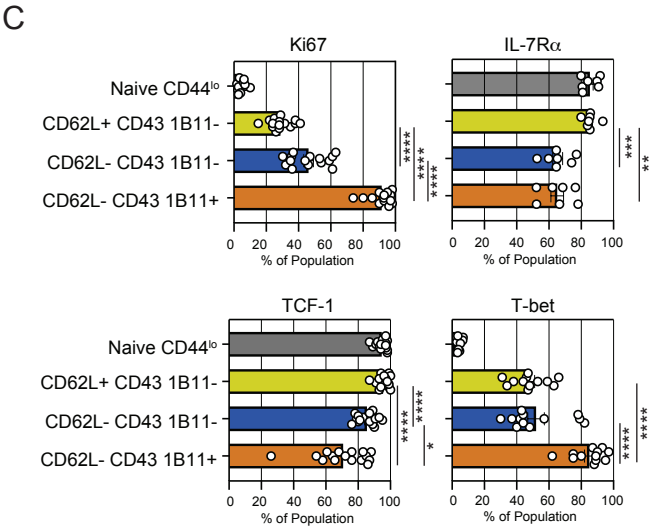
C
Ki67
IL-7Rα
TCF-1
T-bet
Naive CD44lo
CD62L+ CD43 1B11-
CD62L- CD43 1B11-
CD62L- CD43 1B11+
0 20 40 60 80 100
% of Population
****
***
**
*

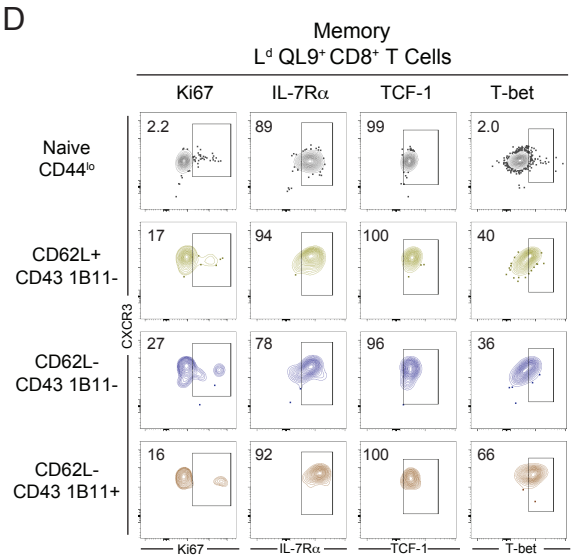
D
Memory
Ld QL9+ CD8+ T Cells
Ki67
IL-7Rα
TCF-1
T-bet
Naive
CD44lo
CD62L+
CD43 1B11-
CD62L-
CD43 1B11-
CD62L-
CD43 1B11+
CXCR3
2.2
89
99
2.0
17
94
100
40
27
78
96
36
16
92
100
66

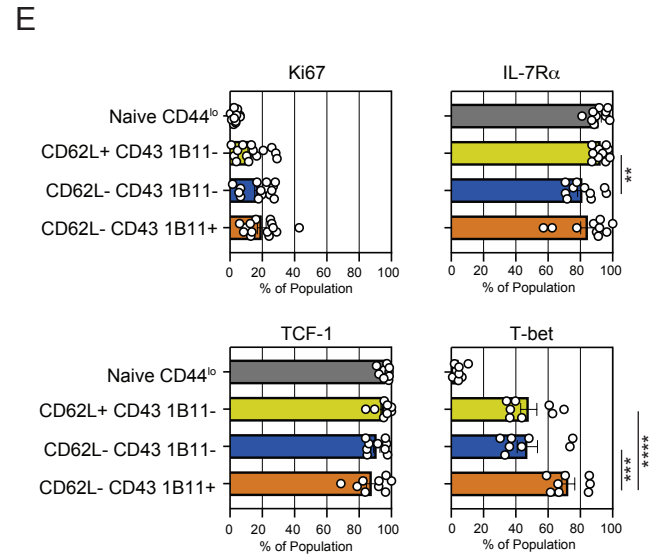
E
Ki67
IL-7Rα
TCF-1
T-bet
Naive CD44lo
CD62L+ CD43 1B11-
CD62L- CD43 1B11-
CD62L- CD43 1B11+
0 20 40 60 80 100
% of Population
**
***
****

Figure 4

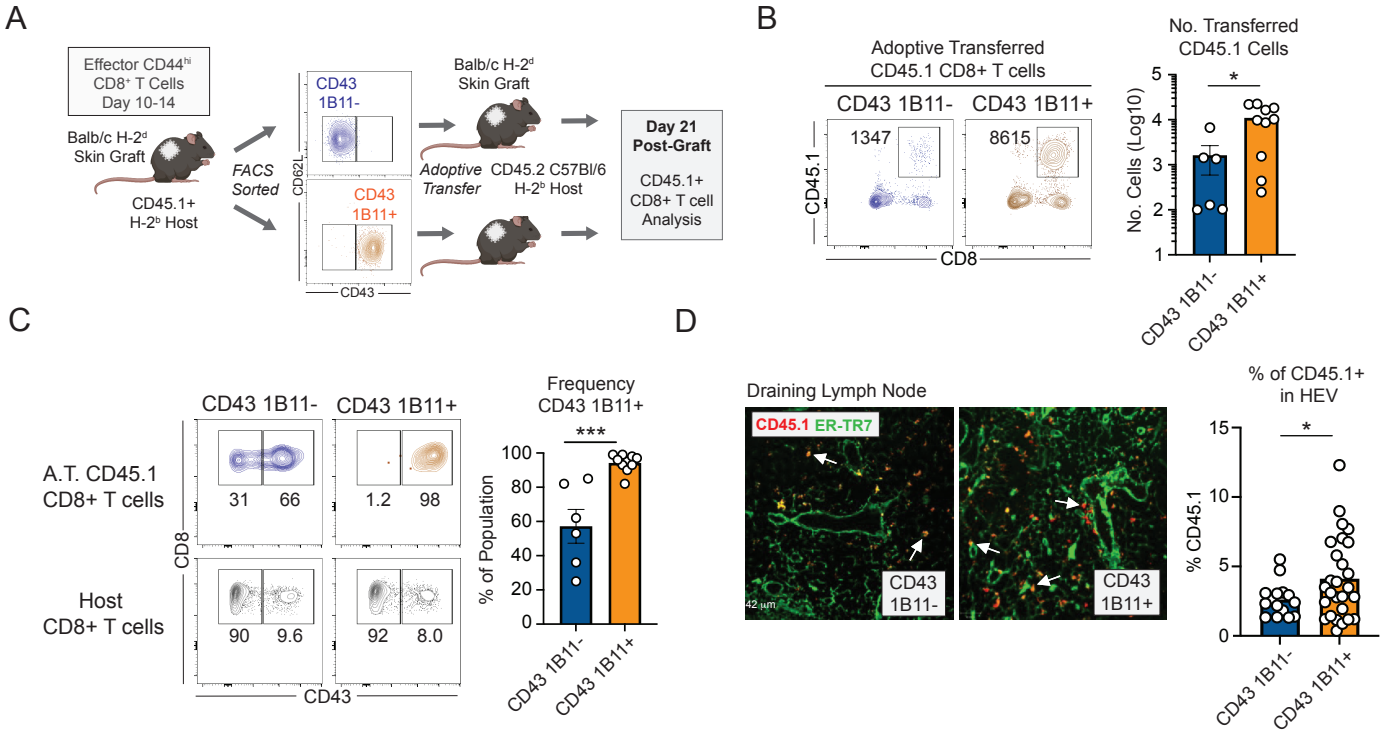
A
Effector CD44hi CD8+ T Cells Day 10-14
Balb/c H-2d Skin Graft
CD45.1+ H-2b Host
FACS Sorted
CD43 1B11-
CD43 1B11+
CD62L
CD43
Balb/c H-2d Skin Graft
Adoptive Transfer
CD45.2 C57Bl/6 H-2b Host
Day 21 Post-Graft
CD45.1+ CD8+ T cell Analysis
B
Adoptive Transferred CD45.1 CD8+ T cells
CD43 1B11-
CD43 1B11+
1347
8615
CD45.1
CD8
No. Transferred CD45.1 Cells
No. Cells (Log10)
*
C
CD43 1B11-
CD43 1B11+
A.T. CD45.1 CD8+ T cells
Host CD8+ T cells
31
66
1.2
98
90
9.6
92
8.0
CD8
CD43
Frequency CD43 1B11+
***
% of Population
D
Draining Lymph Node
CD45.1 ER-TR7
CD43 1B11-
CD43 1B11+
% of CD45.1+ in HEV
*
% CD45.1

Figure 5

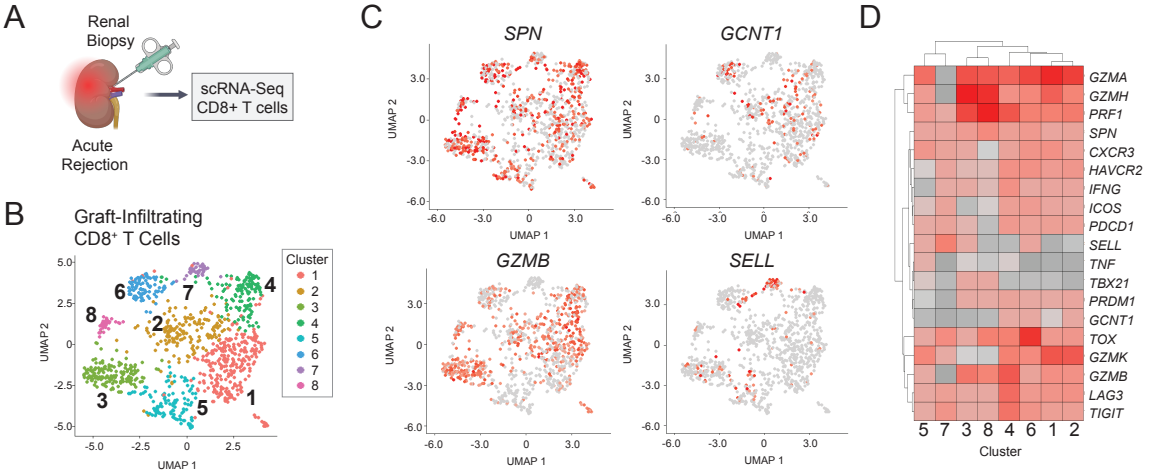
A
Renal Biopsy
scRNA-Seq CD8+ T cells
Acute Rejection
B
Graft-Infiltrating CD8⁺ T Cells
Cluster
1
2
3
4
5
6
7
8
UMAP 1
UMAP 2
C
SPN
GCNT1
GZMB
SELL
D
GZMA
GZMH
PRF1
SPN
CXCR3
HAVCR2
IFNG
ICOS
PDCD1
SELL
TNF
TBX21
PRDM1
GCNT1
TOX
GZMK
GZMB
LAG3
TIGIT
5 7 3 8 4 6 1 2
Cluster

Figure 6

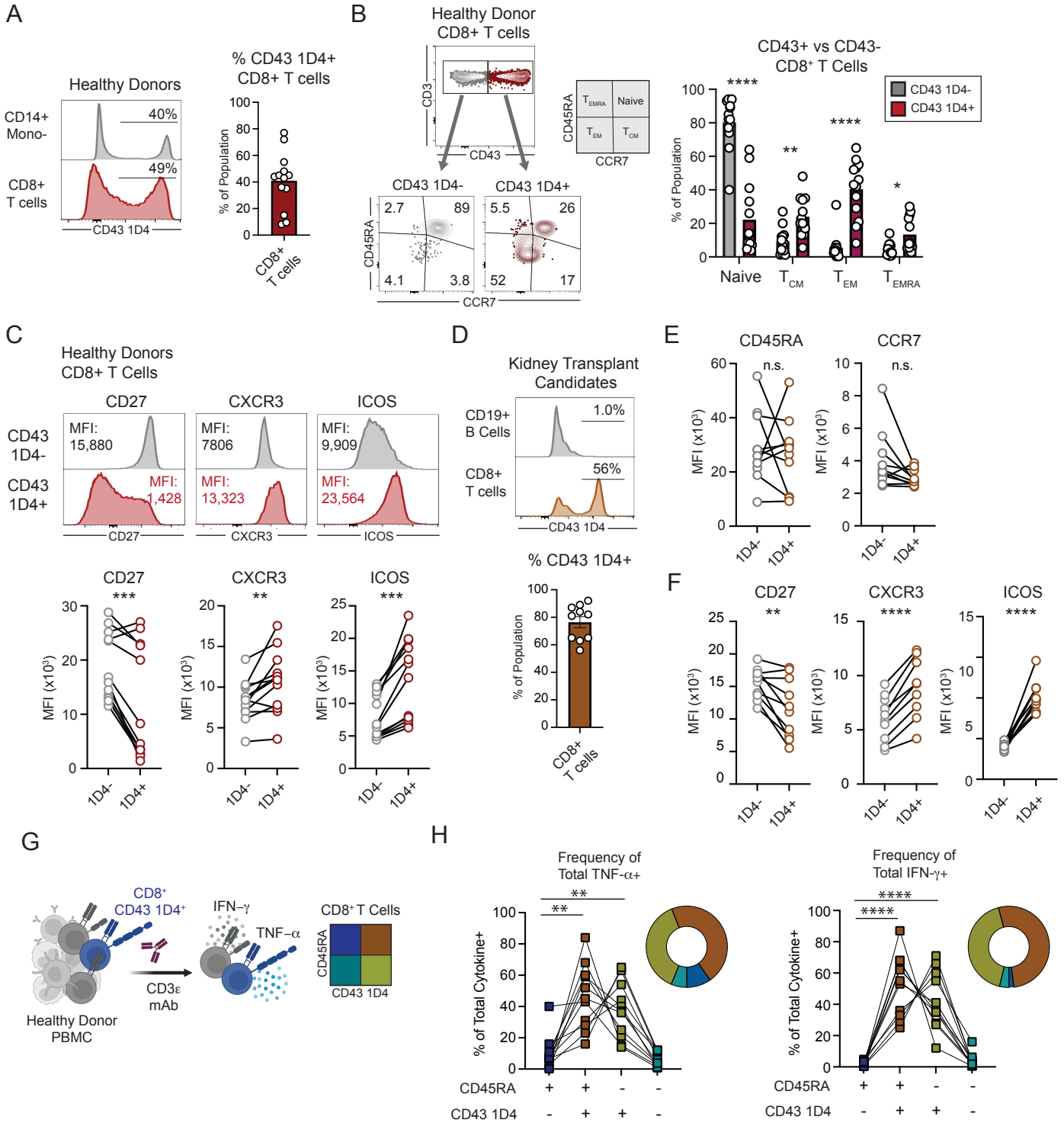
A
Healthy Donors
CD14+ Mono-
CD8+ T cells
40%
49%
CD43 1D4
% CD43 1D4+ CD8+ T cells
% of Population
CD8+ T cells
B
Healthy Donor CD8+ T cells
CD3
CD43
CD45RA
CCR7
Naive
CD43 1D4-
CD43 1D4+
2.7
89
4.1
3.8
5.5
26
52
17
CD43+ vs CD43- CD8+ T Cells
CD43 1D4-
CD43 1D4+
Naive
C
Healthy Donors CD8+ T Cells
CD27
CXCR3
ICOS
MFI: 15,880
MFI: 1,428
MFI: 7806
MFI: 13,323
MFI: 9,909
MFI: 23,564
MFI (x10³)
1D4-
1D4+
D
Kidney Transplant Candidates
CD19+ B Cells
CD8+ T cells
1.0%
56%
% CD43 1D4+
E
CD45RA
CCR7
n.s.
F
G
CD8+ CD43 1D4+
IFN-γ
TNF-α
CD3ε mAb
Healthy Donor PBMC
CD8+ T Cells
H
Frequency of Total TNF-α+
Frequency of Total IFN-γ+
% of Total Cytokine+
CD45RA
CD43 1D4

Figure S1

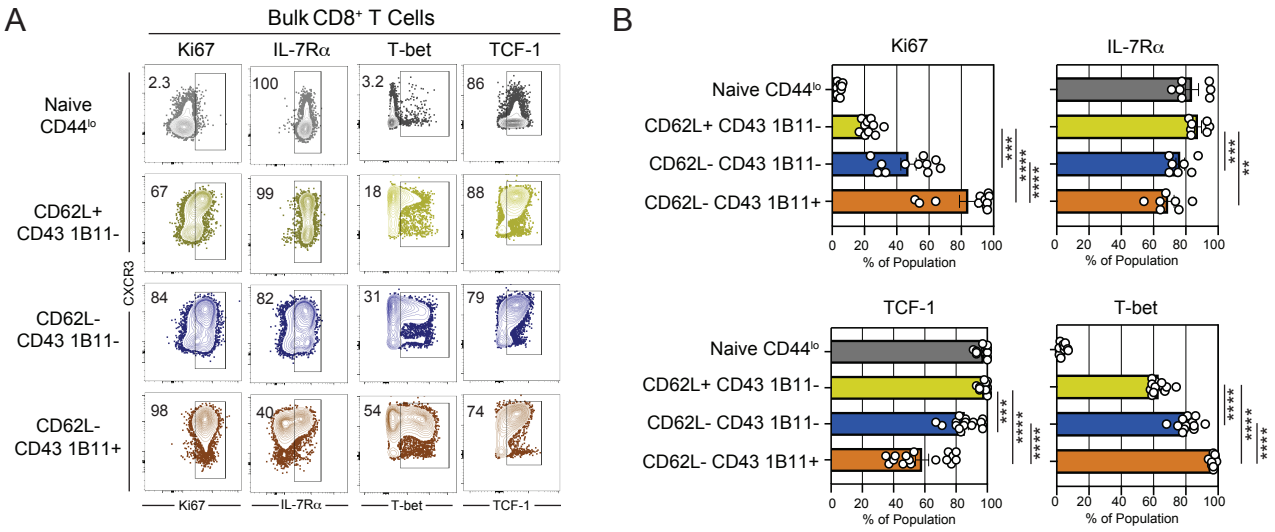
A
Bulk CD8+ T Cells
Ki67
IL-7Rα
T-bet
TCF-1
Naive CD44lo
CD62L+ CD43 1B11-
CD62L- CD43 1B11-
CD62L- CD43 1B11+
CXCR3
2.3
100
3.2
86
67
99
18
88
84
82
31
79
98
40
54
74
B
% of Population
0 20 40 60 80 100
***
****
**

Figure S2

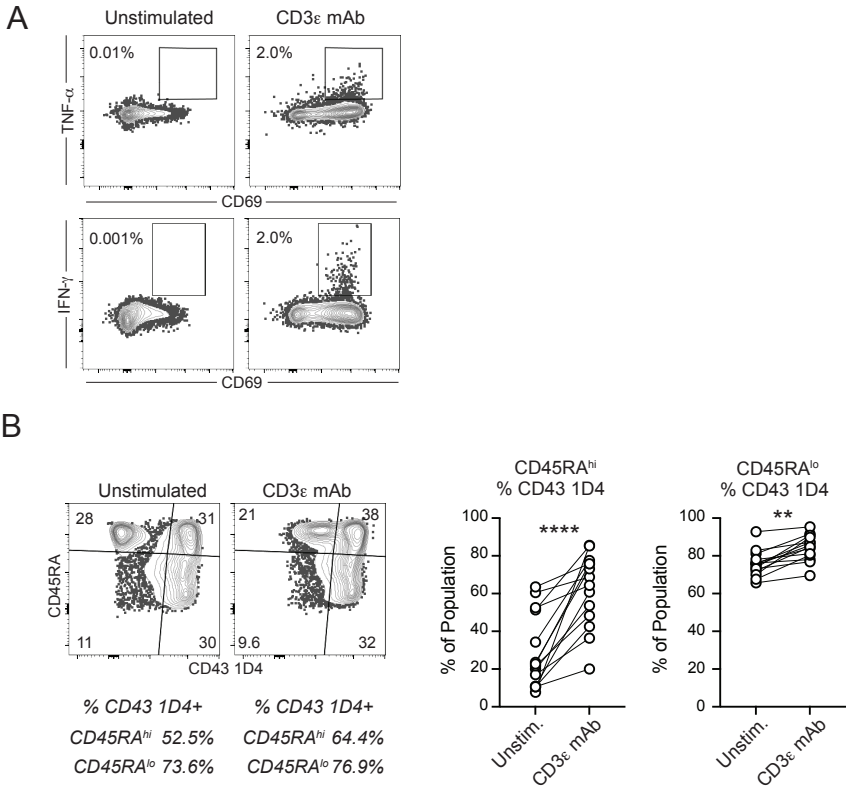
A
Unstimulated
CD3ε mAb
0.01%
2.0%
TNF-α
CD69
0.001%
2.0%
IFN-γ
CD69
B
Unstimulated
CD3ε mAb
28
31
11
30
21
38
9.6
32
CD45RA
CD43 1D4
% CD43 1D4+
CD45RAhi 52.5%
CD45RAlo 73.6%
% CD43 1D4+
CD45RAhi 64.4%
CD45RAlo 76.9%
CD45RAhi
% CD43 1D4
****
% of Population
100
80
60
40
20
0
Unstim.
CD3ε mAb
CD45RAlo
% CD43 1D4
**
% of Population
100
80
60
40
20
0
Unstim.
CD3ε mAb